Characteristics of Pd adsorption on the MgO(100) surface: Role of oxygen vacancies

Livia Giordano,[1] Jacek Goniakowski,[2] and Gianfranco Pacchioni[1]
[1]*Dipartimento di Scienza dei Materiali, Universitá di Milano-Bicocca, Istituto Nazionale per la Fisica della Materia, Via Cozzi, 53, 20125 Milano, Italy*
[2]*Centre de Recherche sur les Mécanismes de la Croissance Cristalline, CNRS, Campus de Luminy Case 913, 13288 Marseille Cedex 9, France*
(Received 6 December 2000; published 27 July 2001)

Using the *ab initio* full-potential linearized augmented-plane-wave approach, we have studied the role of surface oxygen vacancies on the characteristics of palladium deposition on the MgO (100) surface. In agreement with recent theoretical evidence, we find that the adsorption energy of a single Pd atom is considerably enhanced by the defects, and that an important electron transfer from the substrate towards the adsorbed Pd atom occurs. By considering three types of palladium deposits—a single atom, a monolayer, and a bilayer—we have analyzed the evolution of the vacancy-induced interface properties as a function of the dimensionality of the deposit and we show that the modifications reported for the isolated Pd adatoms are to a large extent present also for more extended deposits. However, the electron transfer across the interface remains localized to the close vicinity of the oxygen vacancy, and the stabilization effect of vacancies is particularly strong on lower-coordinated metal atoms. This indicates that the major vacancy-induced modification of the deposit shall be limited to those metal atoms at the cluster edges that adsorb directly at the vacancies.

DOI: 10.1103/PhysRevB.64.075417 PACS number(s): 73.20.At, 68.35.−p, 71.15.Mb

I. INTRODUCTION

The microscopic processes determining the structural, electronic, and growth properties of metal deposits on the insulating, ionic substrates have attracted the growing attention of material scientists both from experimental and theoretical communities. This is partially due to the known but not yet fully understood catalytic properties of supported metal clusters, but also, on a more fundamental level, to the fact that the microscopic description of the interactions on the metal/oxide interface is still far from being complete.[1–9]

The MgO (100) surface is a particularly promising substrate for both fundamental and technological reasons.[1] Experimentally it is relatively easy to prepare single-crystal samples of well-defined surface structure and stoichiometry.[10] Additionally, the high degree of ionicity, the rigidity of the crystalline structure, and the resulting relatively simple atomic structure of the interface justify the abundance of studies on metal deposition on the MgO (100) surface.[6,7] On the other hand, the theoretical studies that have appeared in recent years have helped the analysis and interpretation of experimental results, have elucidated many basic questions, and validated to a large extent the existing state of the art of quantum-mechanical approaches as adequate for the description of adsorption[11–14] and growth[15,16] of metals on an oxide substrate.

The existing studies have principally focused on the perfect interfaces and it is only very recently that the extension towards a controlled analysis of the role of surface point defects has been attempted.[15,17,18] Very recent atomic force microscopy (AFM) experiments have shown that the nucleation kinetics is governed by point defects with a high trapping energy.[19] The peculiar catalytic properties of supported gold clusters have been tentatively attributed to vacancy-induced modification of the electronic properties of the deposited metal clusters.[20] In fact, theoretical studies reveal an important increase of the adsorption energy of metal adatoms and a considerable electron transfer between the substrate and the adsorbate induced by surface oxygen vacancies.[15,21–24] However, the existing results concern principally the isolated adatoms or adsorbed dimers and are thus representative of the very early stages of cluster growth. At present, it is not at all clear to what extent the reported strong modifications of adsorption characteristics can affect the adhesion and the electronic properties of more extended deposits.

The goal of the present paper is thus to analyze the evolution of the vacancy-induced modifications of the characteristics of metal adsorption as a function of the dimensionality of metal deposits. We will focus on the adsorption energetics, on the related modifications of the interface adhesion energy, and on the charge transfer between the substrate and the adsorbate. To this end, we have chosen to analyze three model metal deposits, namely an isolated atom, an epitaxial monolayer, and an epitaxial bilayer, in each case comparing the adsorption characteristics obtained for the deposition on the regular and on the oxygen-deficient MgO (100) surface. The three systems have the advantage of covering in a systematic fashion the metal-metal coordination numbers ranging from an isolated adatom to a fully constituted metal/MgO(100) interface, and to model zero-, two-, and three-dimensional deposits, respectively. This choice, although it does not allow for a direct comparison with a particular set of experimental results, has the advantage of giving a relatively clear physical picture of microscopic mechanisms responsible for the analyzed effects and facilitates the elaboration of general physical conclusions. In this way, it constitutes a definite basis for further experimental and theoretical studies.

The paper is organized as follows. In Sec. II, we briefly describe the computational settings used for the present study. Section III starts with a presentation of the model of

the oxygen-deficient MgO (100) surface used in the study, and then summarizes the numerical results concerning the palladium adsorption characteristics. In Sec. IV, we discuss the results and derive some general trends in adsorption energetics and interface charge transfer.

II. TECHNIQUES

The present study makes use of the density-functional-based, full-potential linearized augmented-plane-wave (FP-LAPW) method,[25] which has already been successfully applied to studies on surface processes and metal-oxide interfaces.[26,27] In order to better account for adsorption energetics, we have used the generalized gradient approximation (GGA), which has proven its reliability for study of metal-atom adsorption on oxides, as well as for the particular case of Pd on the MgO (100) surface.[13] Recent studies on vacancies in metals[28] or metal/alumina interfaces[29] suggest that the performance of the GGA is not equally satisfactory for all physical systems. However, for the Pd/MgO(100) interface, the excellent agreement between the present results and the full-potential linear-muffin-tin-orbital (FP-LMTO) local-density-approximation (LDA) findings by Goniakowski[30] tends to prove that the different choice of the exchange-correlation potential will not modify the principal physical conclusions of the study. We have used the GGA functional in the form proposed by Perdew and Wang.[31]

Within the FP-LAPW method, space is divided into non-overlapping spheres centered on the atomic sites. Spheres of 1.9 a.u. radius were used for oxygen and magnesium atoms and spheres of 2.0 a.u. radius for palladium. The basis set consists of plane-wave envelope functions that are augmented inside the atomic spheres by means of a numerical solution of the Schrödinger equation. Partial waves up to $l=10$ are used inside the atomic spheres. We have added the so-called ''local orbitals'' in order to include the 2*s* electrons of O, 2*s* and 2*p* electrons of Mg, and 4*p* electrons of Pd as semicore states. The convergence of the basis set is controlled by a cutoff parameter $R_{\mathrm{mt}}K_{\mathrm{max}}$, which was set equal to 6 (10 Ry) during the geometry optimization. Calculations with the cutoff increased to 10 (28 Ry) were made for all the optimized geometries in order to estimate the adsorption energies, charge distributions, and densities of states.

Tests on the adequacy of this computational approach for representation of bulk Pd and MgO and of their surfaces were reported in Ref. 32. In the present calculations, the MgO surface is represented by a three-layer-thick unrelaxed MgO slab of theoretical bulk MgO lattice constant (4.26 Å) and (2×2) surface unit cell. Pd was adsorbed symmetrically on both sides of the slab. We will discuss the validity of this surface model in the next section. Two-dimensional **k**-point sampling of the Brillouin zone is converged to within 0.1 eV per atom (with a Gaussian broadening of 2 mRy). This is achieved with six **k** points in the irreducible part of the Brillouin zone (BZ). In order to compensate for the possible lack of full convergence with respect to computational settings, all calculations necessary for the determination of adsorption energies were performed with exactly the same periodic supercell.

III. RESULTS

We start with a brief presentation of the atomic and the electronic structures of the regular and of the oxygen-deficient MgO (100) surfaces. Later on, we report the results of calculations on the adsorption of different palladium deposits. In each case, we present a comparison of calculated electronic and atomic structures for adsorption on the regular and the oxygen-deficient surfaces.

A. Oxygen vacancies on the MgO (100) surface

The existing studies on oxygen vacancies on the MgO(100) surface indicate that the interaction between the surface vacancies is relatively weak and that it decreases rapidly as a function of the distance between the vacancies. In particular, between the 12.5% and 25% coverage of surface oxygen vacancies, the formation energy changes by less than 5%.[33] Furthermore, both structural and energetic contributions due to the surface relaxation are small: the relaxation energy is of the order of 0.1 eV,[22,33] and the related atomic displacements are of the order of 0.05 Å.[33] We have chosen the 25% oxygen-deficient unrelaxed surface (the lateral vacancy-vacancy nearest-neighbor distance of 6 Å) as a representation of an isolated oxygen vacancy. In the following, we will refer to this model as the oxygen-deficient surface. In order to test the effect of limited slab thickness, we have compared the adsorption energetics of the Pd monolayer deposited on the fully oxygen-deficient MgO (100) surface, represented either by a three-layer-thick slab or by a five-layer-thick slab. The difference between the adsorption energies in the two cases did not exceed 0.03 eV/Pd at, showing that the three-layer slab is an adequate representation of the oxygen-deficient surface.

Within these settings, the vacancy formation energy calculated with respect to a free oxygen atom in its spin-polarized ground state is 9.5 eV. This can be compared to the existing results of the plane-wave, periodic LDA calculations by Kantorovich *et al.*[34] and Finocchi *et al.*[33] who, for the same concentration of vacancies, report, respectively, 9.8 and 10.2 eV. GGA calculations by Bogicevic and Jennison,[15] well converged with respect to the size of the supercell, give 9.6 eV. Hartree-Fock calculations reported in Ref. 35 estimate the formation energy of an isolated vacancy to be 7.8–8.1 eV. Embedded Møller-Plesset perturbation theory up to the second order calculations by Scorza *et al.* predict 9.35 eV.[36] Satisfactory agreement with the existing results shows that the effect of limited slab thickness on the vacancy formation energy is relatively small.

Figure 1 presents the valence-band densities of states (DOS) calculated for the perfect and the oxygen-deficient MgO (100) surfaces. Projection on the surface oxygen atoms is plotted separately. The projection procedure, although dependent on the choice of the atomic spheres, has the advantage of elucidating the origin of different structures in the total DOS. In all the graphs, the energy scales are shifted so as to align the DOS projected on the atoms of the central layer of the slab (not shown in the figure). In both cases, the Fermi level is placed at the highest occupied state in order to show clearly the vacancy-induced occupied states in the gap.

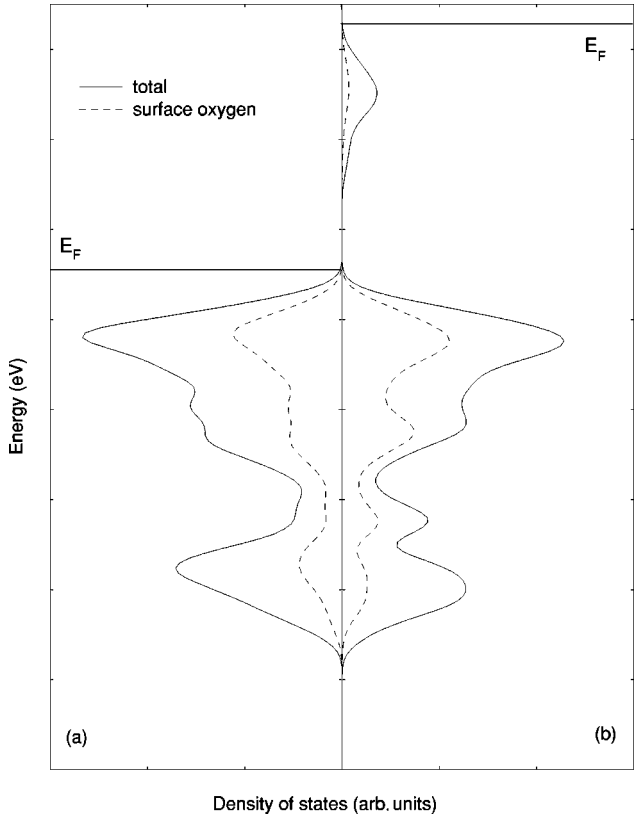

FIG. 1. Valence-band DOS for the regular (a) and the oxygen-deficient (b) MgO (100) surface. Total DOS together with projection on the surface oxygen atoms are plotted. All DOS have been convoluted with a 0.1-eV-wide Gaussian function.

Since the position of the origin of the energy axis is arbitrary, the corresponding tick marks are not labeled explicitly.

The valence band of the clean MgO (100) surface has principally oxygen $2p$ character. Due to a weakening of the Madelung field at the surface, the contribution of the surface oxygen atoms is shifted towards higher energies with respect to the bulk (center of the slab). The principal modification introduced by the surface vacancies is the appearance of occupied electronic states in the gap. This new feature in the band structure corresponds to two electrons left on the surface when a neutral oxygen atom is extracted. The detailed analysis of the related wave functions and charge densities shows that these two electrons remain relatively well localized at the vacancy site.[21,33,34,36,37] In the present case, the vacancy states form a narrow band (1.8 eV) positioned 2.0 eV above the bulk valence-band maximum (VBM). This can be directly compared to the band between 1.7 and 3.2 eV above the VBM reported in Ref. 33 and to that at about 2.3 eV above the VBM reported in Ref. 34. As was clearly shown in Ref. 33, the position and the width of the vacancy band depend on the vacancy concentration. In fact, 12.5% of the surface vacancies produce a nearly nondispersive band at about 2 eV above the VBM. The broadening visible in the present calculations is principally due to the lateral interactions between the vacancies. As for the vacancy-formation energetics, this comparison shows that the effect of the slab thickness on the electronic properties of the vacancy is practically negligible.

TABLE I. Adsorption properties of an isolated Pd atom on the regular and on the oxygen-deficient MgO (100) surface: adsorption energy E_{ads} (eV), Pd-surface distance d (Å).

	E_{ads}	d
Regular	1.43	2.13
Oxygen-deficient	3.73	1.44

B. Adsorption of an isolated Pd atom

We proceed to the results on the adsorption of an isolated Pd atom on the regular and on the oxygen-deficient MgO(100) surfaces. In order to represent an isolated atom in the periodic calculations, we adsorb a single Pd per (2×2) surface unit cell symmetrically on each side of the slab. This corresponds to $\frac{1}{4}$ Pd ML coverage, and to the nearest-neighbor Pd-Pd distance of 6 Å. At this distance, the direct interaction between Pd atoms is negligible. For the regular MgO (100) surface, only the most stable oxygen adsorption site, as determined both theoretically and experimentally, is considered.[38–41] Since the plane-wave calculations[42] show that a full optimization of geometry changes the calculated adsorption energy by 5% only, and modifies the adsorption height by less than 2%, in the following we will thus systematically neglect relaxation of the substrate.

In general, the adsorption energy with respect to free Pd atoms can be estimated through

$$E_{\mathrm{ads}}=-\frac{1}{2N}(E^{\mathrm{Pd/MgO}}-E^{\mathrm{MgO}}-2NE^{\mathrm{Pd}}_{\mathrm{atom}}),$$

with $E^{\mathrm{Pd/MgO}}$, E^{MgO}, and $E^{\mathrm{Pd}}_{\mathrm{atom}}$ being the total energies of the MgO slab with N Pd atoms adsorbed symmetrically on each side, of the clean MgO slab, and of a free Pd atom, respectively. In the present case, $N=1$, but the same formula will be further used with $N=4$ and $N=8$ for the cases of adsorption of a monolayer and of a bilayer. Calculated adsorption heights and binding energies are shown in Table I.

As far as adsorption on the regular surface is concerned, our results are fully consistent with the data existing in the literature. Periodic[30] and cluster[22] calculations give, respectively, $E_{\mathrm{ads}}=1.3$ eV ($d=2.08$ Å) and 1.35 eV (2.11 Å). Satisfactory agreement between the periodic and cluster results confirms the adequacy of the present, $\frac{1}{4}$ Pd ML model to represent isolated Pd adatoms.

With respect to the regular MgO(100) surface, the presence of an oxygen vacancy very clearly stabilizes the adsorption. To our knowledge, only two studies of the adsorption of an isolated Pd atom on an oxygen vacancy have been reported in the literature. Our results are in excellent agreement with those of Matveev *et al.*,[22] who, using an embedded cluster approach within the Becke-Perdew gradient-corrected density-functional-theory (DFT) method, found the Pd atom bound by 3.76 eV at 1.53 Å above an isolated oxygen vacancy. On the contrary, our results differ considerably from those of Ref. 21, where the Hartree-Fock (HF) -based embedded cluster approach gives an adsorption energy of 1.55 eV and an adsorption height of 1.73 Å. In this latter case, the underestimation of bond strength is mainly due to the lack of

correlation effects but also to an embedding scheme that did not include effective core potentials to avoid the unphysical polarization of the oxygen atoms at the cluster border.

It is worth mentioning that very similar calculations on Ag adsorption on the regular and oxygen-deficient surfaces have been recently performed within an equivalent periodic slab approach[24] and within a cluster model.[22] Although these two sets of results are not directly comparable because the approximations on the electronic interactions employed by the two groups are not the same (Hartree-Fock and DFT, respectively), the adsorption energy of an isolated Ag adatom on the vacancy given by the periodic HF approach[24] is nearly five times bigger than the energy given by the cluster DFT calculations.[22] The authors of Ref. 24 tend to attribute this important difference to two effects: possible deficiencies of the embedding scheme used in the cluster calculations, or a possible interaction between the periodic images in the slab calculations. We belive that the excellent agreement between our periodic-slab results and the results of cluster calculations by Matveev *et al.*[22] shows the perfect equivalence of the two qualitatively different methods for description of the surface processes.

From an experimental point of view, using a rate equation model to describe the nucleation process of Pd on MgO observed by AFM, Haas *et al.*[19] estimate an adsorption energy to about 1.2 eV for regular sites and a trapping energy to somewhat more than 1.5 eV for the surface defects. Taking into account the good agreement between the experimental and theoretical estimation of adsorption energy at the regular surface, the important difference between the calculated adsorption energy for Pd at an oxygen vacancy and the experimental trapping energy suggests that they are not oxygen vacancies that have been observed experimentally. The nature of these defects has not yet been unambiguously identified.

The important difference between the adsorption characteristics of Pd atoms on the regular and oxygen-deficient surfaces can be related to the vacancy-induced modifications of the electronic structure. In Fig. 2, we show the valence-band DOS calculated for the two cases. Projections on the Pd atom and on surface oxygen are plotted separately.

Two qualitative differences in the DOS of the adsorbate should be stressed. First, the position of the Pd level with respect to the substrate valence band changes as a function of the adsorption site. When adsorbed on the surface oxygen, this level is well above the MgO valence band, whereas the two intersect when Pd is adsorbed above the surface vacancy. An increase of the Pd bandwidth and a downward shift of its center of gravity contribute to this effect. Second, the character of the Pd band changes. When adsorbed above the surface oxygen, the 5*s* and 4*d* components are clearly separated, and the occupied Pd band has a strong *d* character. When adsorbed above the vacancy, the two components hybridize. A rough inspection of the corresponding DOS reveals that the electronic population of the Pd atom is bigger when adsorbed at the vacancy. We will propose a quantitative electron counting scheme in the next section.

As already pointed out by the authors of Ref. 21 and Ref. 22, the increase of the adsorption energy on the vacancy can

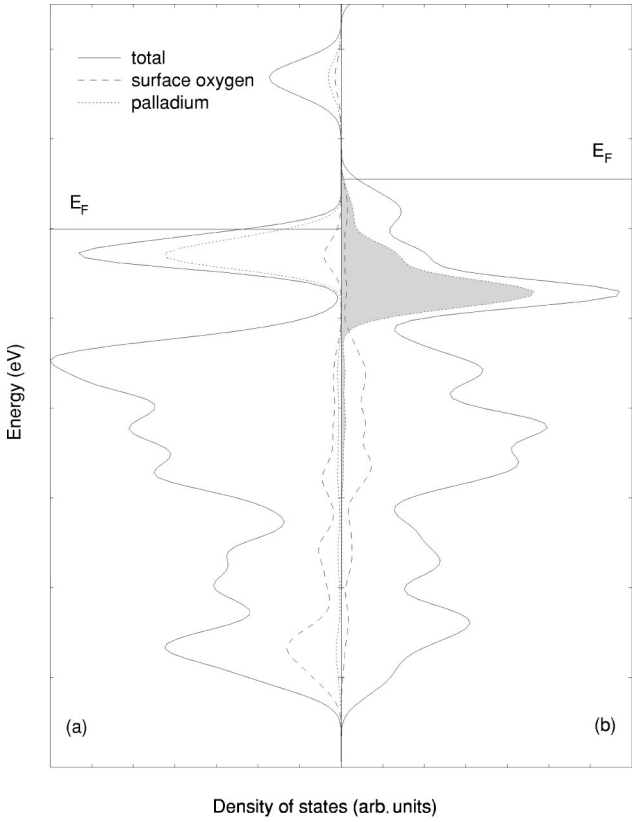

FIG. 2. Valence-band DOS of an isolated Pd atom adsorbed on the regular (a) and on the oxygen-deficient (b) MgO (100) surface. Projections on the surface oxygen and on the Pd atom at the regular (clear) and at the vacancy (shaded) sites are plotted. All DOS have been convoluted by a 0.1-eV-wide Gaussian function.

be related to two principal factors. First, the strong hybridization between the Pd and the vacancy state lowers the position of the vacancy state and enhances the *s*-*d* hybridization of the Pd outer shells. Second, in the absence of the surface oxygen atom, the Pauli repulsion decreases considerably.

C. Adsorption of a palladium monolayer

We proceed to the presentation of the results of the deposition of an epitaxial Pd monolayer, which, with respect to the zero-dimensional, isolated Pd adatoms, represents a model two-dimensional deposit. Again, the (2×2) surface cell, this time with four Pd atoms adsorbed at each side of the slab, was used. Respecting the model character of the considered metal deposits and preserving the epitaxial structure of the interface, we optimize only the vertical positions of the Pd atoms.

On the regular surface, as can be seen in Tables II and I, the increase of Pd coverage induces an important increase of the adsorption energy. This is mostly due to the additional Pd-Pd bonds within the monolayer, the interaction between the Pd and the substrate being weaker.[30]

The presence of the vacancy further increases the adsorption energy. The numbers given in Table II correspond to an average over four inequivalent Pd atoms of the (2×2) sur-

TABLE II. Adsorption properties of an epitaxial Pd monolayer deposited on the regular and on the oxygen-deficient MgO(100) surface: average adsorption energy per Pd atom $\langle E_{ads} \rangle$ (eV), average Pd-surface distance $\langle d \rangle$ (Å), corrugation of the Pd layer Δd (Å).

	$\langle E_{ads} \rangle$	$\langle d \rangle$	Δd
Regular	2.15	2.21	0.00
Oxygen-deficient	2.57	2.00	0.66

face cell, one that is adsorbed at the vacancy and the remaining three that are adsorbed at the neighboring regular surface sites. An alternative way to look at the energy would consist in a calculation of the gain induced by the vacancy, which can be estimated to be 1.68 eV/surface cell. This value, much smaller than the corresponding result for the adsorption of isolated atoms (2.30 eV), suggests that although it exists, the stabilization effect of the vacancy weakens considerably in the presence of an extended deposit. The effect of weakening of the deposit-substrate interactions as a function of increasing coordination number of atoms within the deposit, typical for interactions of many-body character, was already reported for Pd deposited on the regular MgO(100) surface.[30]

The presence of the vacancy causes a corrugation of the adsorbed Pd film: the atom at the vacancy site adsorbs relatively close to the surface (1.53 Å); its neighbors at the regular sites adsorb at a somewhat higher distance (2.19 Å). Clearly, the interactions within the monolayer make the resulting corrugation (0.66 Å) considerably smaller than the difference between the adsorption heights of an isolated atom at the vacancy and an atom within 1 ML on the regular surface (0.77 Å). At the same time, the balance of Pd-vacancy and Pd-Pd interactions results in an increased adsorption height of Pd at the vacancy with respect to the case of an isolated atom. The structural results show very clearly that the vacancy-induced modifications within the deposited Pd layer go beyond the second Pd neighbors, and suggest that the (2×2) surface unit cell is not large enough to avoid completely the metal-mediated interactions between the periodic images of the vacancy.

As far as the DOS for the regular surface is concerned, two principal effects are clearly visible in Fig. 3. With respect to the adsorption of an isolated atom, the width of the Pd band and the hybridization between the *s* and *d* components increases. On the other hand, the Pd-O hybridization is considerably smaller. Both these effects reflect an important intralayer bonding and a reduction of the metal-oxide interactions.[30]

When an oxygen vacancy is present, the Pd atoms within the layer become inequivalent, and the corresponding Pd-projected DOS changes considerably. The contribution of the Pd atom adsorbed at the vacancy is shifted downwards on the energy scale, and its width is considerably reduced. The electronic population at this particular atom is higher, indicating an electron transfer from the vacancy. The reduced width of its DOS reflects a small hybridization with the rest of the layer and suggests a high degree of localization of the transferred electrons.

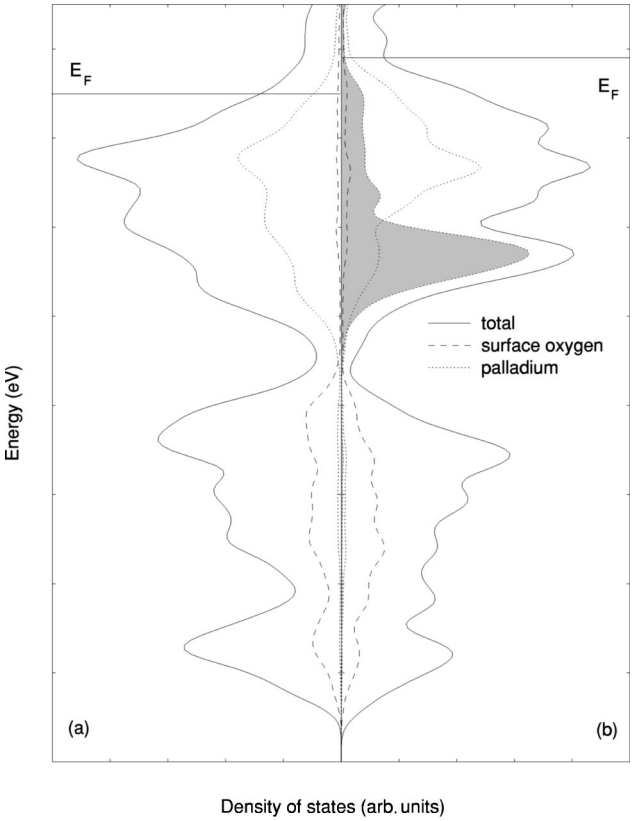

FIG. 3. DOS for a Pd monolayer adsorbed on the regular (a) and on the oxygen-deficient (b) MgO(100) surface. Total DOS and projections on the surface oxygen and on the Pd atom at the regular (clear) and at the vacancy (shaded) sites are plotted. All DOS have been convoluted by a 0.1-eV-wide Gaussian function.

D. Adsorption of a palladium bilayer

We turn now to the adsorption of an epitaxial Pd bilayer, which can be considered as the simplest model of a three-dimensional deposit. As before, we use the (2×2) surface unit cell, we preserve the fcc structure of Pd, expand its lateral lattice parameters so as to match those of MgO, and optimize the vertical positions of all Pd atoms. Table III summarizes the structural and energetic characteristic of Pd bilayer deposition on the regular and on the oxygen-deficient MgO (100) surfaces.

On the regular surface, if compared to the 1-ML deposit, we observe a further, small increase of the adsorption energy. Remembering that at present the energy is averaged over the

TABLE III. Adsorption properties of Pd bilayer deposited on the regular and on the oxygen-deficient MgO(100) surface: average adsorption energy per Pd atom E_{ads} (eV), average adsorption height $\langle d_1 \rangle$ (Å), average distance between Pd layers $\langle d_2 \rangle$ (Å), and the corrugation of the interface and of the second Pd layer Δd_1 and Δd_2 (Å).

	$\langle E_{ads} \rangle$	$\langle d_1 \rangle$, $\langle d_2 \rangle$	Δd_1, Δd_2
Regular	2.91	2.34, 1.73	0.00, 0.00
Oxygen-deficient	3.04	2.12, 1.74	0.43, 0.00

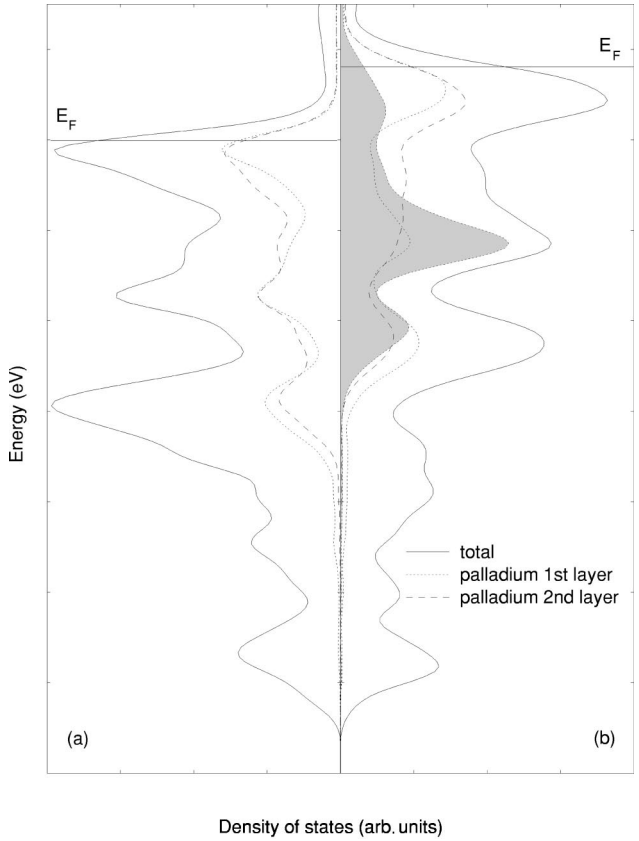

FIG. 4. DOS of a Pd bilayer adsorbed on a regular (a) and on the oxygen-deficient (b) MgO(100) surface. Total DOS and projections on the Pd atoms at the regular (clear) and at the vacancy (shaded) sites are plotted. All DOS have been convoluted by a 0.1-eV-wide Gaussian function.

Pd atoms at the interface and in the second layer, its increase can be principally related to the increase of the coordination of Pd atoms within the deposit. The interaction between the substrate and the adsorbate has a tendency to weaken further.[30]

The presence of the vacancy changes the adsorption energy by about 0.1 eV only. The corresponding gain of energy due to the presence of the vacancy amounts to 1.04 eV/surface cell, and reflects a further important weakening of the stabilization effect of the vacancy. In parallel, the adsorption height of the Pd atom directly at the vacancy increases (1.81 Å), and as a consequence, the corrugation of the interfacial layer becomes smaller. However, even in this case the difference between the vertical positions of the Pd atoms at the vacancies and at the regular sites remains of the order of 0.5 Å. The small difference between the interlayer distance $\langle d_2 \rangle$ calculated for the regular and oxygen-deficient interfaces reflects the particularly rapid attenuation of the vacancy-induced modifications in the direction perpendicular to the interface.

As can be seen in Fig. 4, the main modification of the electronic band structure with respect to the 1-ML case consists of an important widening of the Pd band, which in the present case clearly overlaps with the substrate valence band. The vacancy-induced modification of the DOS is small. Although as before the DOS of the Pd atom directly on the vacancy site is shifted towards lower energies and more localized than those of other Pd atoms, one can see its clear hybridization with the rest of the metal band. Contrary to the case of the 1-ML deposit, in the present situation the center of gravity of the LDOS of the atom at the vacancy is situated well within the Pd band.

TABLE IV. Adhesion energy E_{adh} (eV/interface Pd at) of an isolated Pd atom, Pd monolayer, and Pd bilayer on the regular and on the oxygen-deficient MgO(100) surface.

E_{adh}	Pd atom	Pd 1 ML	Pd 2 ML
Regular	1.43	0.58	0.53
Oxygen-deficient	3.73	1.01	0.81

IV. DISCUSSION

In the following, we will focus on two qualitatively different aspects of the vacancy-induced modifications of the Pd/MgO(100) interface. First, we will see to what extent the strong increase of bonding that is found for adsorption of single Pd atoms and that is potentially relevant for the early stages of the metal deposition does influence the adhesion of an extended interface, and thus the equilibrium atomic structure of the deposited clusters. Second, we will analyze more quantitatively the charge transfer between the substrate and the deposited metal and the related electron redistribution within the deposit. Understanding the evolution of the charge transfer as a function of the dimensionality of the deposit may help to understand if the recently proposed arguments relating the particular reactivity of small metal particles to the electron transfer from the surface vacancies remain valid also for extended deposits.

A. Adhesion energy of the interface

In order to analyze the evolution of bonding at the interface, we will supplement the analysis of adsorption energies with respect to free Pd atoms (E_{ads}) by evaluation of adsorption energies with respect to the unsupported Pd deposit (E_{adh}). The former contains information on both Pd-Pd and Pd-MgO interactions, whereas the latter, which can be expressed as

$$E_{\mathrm{adh}} = -\frac{1}{2N}\left(E^{\mathrm{Pd/MgO}} - E^{\mathrm{MgO}} - 2E^{\mathrm{Pd}}_{\mathrm{deposit}}\right)$$

(where $E^{\mathrm{Pd/MgO}}$, E^{MgO}, and $E^{\mathrm{Pd}}_{\mathrm{deposit}}$ are the total energies of the MgO slab with a Pd deposit on each side, of the clean MgO slab, and of an unsupported Pd deposit, respectively, and N is the number of Pd atoms at the interface) gives directly the Pd-MgO contribution and approaches closely the adhesion energy of the interface (see Table IV). Although within these settings the reference for calculations of E_{adh} for the regular and oxygen-deficient interfaces are not precisely the same, we have verified that the difference is of the order of 0.02 eV/at, much smaller than the discussed energetics.

The energetics of Pd deposition on the regular MgO (100) surface as a function of the deposit size has been already discussed in detail and related to the modifications of the electronic structure in Ref. 30. The present results reproduce well the principal tendency, namely the reduction of the interface bonding for more extended deposits, reflecting the many-body character of the interactions. It is worth pointing out that the adhesion energy calculated for the Pd bilayer approaches closely the experimental estimate of 0.51–0.56 eV/Pd at, obtained from the Wulff-Kaishev construction applied to deposited Pd clusters of 10–20-nm size.[43]

As far as the deposition on the oxygen-deficient surfaces is concerned, the adhesion energies are considerably enhanced. Their decrease along the series is principally due to the weakening of the Pd-vacancy interaction, but also to the modification of bonding within the Pd deposit. The substrate-induced changes of cohesion of the deposit were already discussed for the regular surface in Ref. 44, and we return to this question when analyzing the changes of bonding in Pd dimers adsorbed on MgO(100) surface defects.[42]

The vacancy-induced increase of the adhesion energy can be expected to produce a modification of the equilibrium atomic structure of the deposited clusters. A simple argument based on the Wulff theorem and applied to the known, pyramidal form of the Pd deposits on the MgO(100) substrate[6] would suggest a reduction of the cluster height and thus an increase of the proportion of the (100) facets with respect to the (111) ones. This effect, and the related change of edge lengths, will necessarily lead to a modification of the catalytic properties of the deposited clusters. On the other hand, the strong dependence of the stabilization effects of vacancies on the coordination of the metal atoms suggests that the vacancies would preferably occupy the undercoordinated regions of the interface corresponding to the cluster's edges and corners. This observation seems coherent with the atomic structure of the Au clusters on the oxygen-deficient MgO (100) surface as reported by Sanchez *et al.*,[20] where a three-dimensional cluster does not cover the vacancy. Taking this into account, the modification of the reactivity by vacancies at the cluster edges may in fact be the principal experimentally detectable effect. Although the controlled generation of surface defects may seem to be a tool for a fine-tuning of the catalyst's reactivity, one should not forget that the presence of vacancies may also be at the origin of structural defects within the deposit and that it may modify the kinetics of cluster growth and the cluster-size distribution.

B. Electron redistribution at the interface

In order to access the evolution of the charge transfer between the MgO and the Pd deposit as a function of the deposit dimensionality, we have used two complementary techniques. The first one, based on the Bader-like method,[45,32] consists of a partition of space into layers, delimited by the local minima in the electron density profile $\rho(z)=\int\rho(x,y,z)dx\,dy$ along the direction z, perpendicular to the interface. The results of this decomposition can be associated with charges of the subsequent Pd atomic layers, which on the regular surface are directly related to charges of Pd atoms. In the case of adsorption on the oxygen-deficient surface, the electronic occupations of different Pd atoms in the interfacial layer are not the same, so we have performed a supplementary decomposition of the electronic charge distribution $\rho(\mathbf{r})$, consisting this time in the evaluation of the radial electron density function $\rho(r)$ for each Pd atom. We then use the $\int^{r_c}\rho(r)r^2dr$, where r_c corresponds to the minimum of $\rho(r)$, as an estimation of the charge of the particular atomic site (see Table V). It should be stressed that the above decomposition remains arbitrary and we will thus not insist on the precise values of calculated charges. This applies also to what we will call charge transfer and what, within the above decomposition scheme, can be induced by a real electron transfer between atoms, or by a strong polarization of their electronic clouds.

TABLE V. Charges per Pd atom for an isolated Pd atom, a Pd monolayer, and a Pd bilayer deposited on the regular and the oxygen-deficient MgO(100) surfaces. For the Pd bilayer, the first and the second column correspond to the interface and the second Pd layer, respectively. Decomposition over inequivalent Pd atoms within the interface layer is given explicitly.

	Pd atom	Pd 1 ML	Pd 2 ML	
Regular	−0.36	−0.13	−0.08	−0.02
Oxygen-deficient	−0.86	−0.93, −0.01	−0.63, −0.03	−0.01

When palladium is deposited on the regular surface, the electron transfer from the substrate to the adsorbate is relatively small and it clearly decreases as a function of the Pd coverage. Both its direction and its evolution are fully coherent with the microscopic model proposed in Ref. 30, according to which the formation of Pd-O bonds pushes the antibonding oxygen states above the Fermi level and results in an electron transfer towards Pd. Furthermore, since the Pd-O bonding becomes weaker when Pd gains its metal neighbors, this electron transfer diminishes. In the case of adsorption of an isolated Pd atom, a similarly small electron transfer was found by Matveev *et al.*[22]

When a vacancy is present, the electron transfer from the substrate to the adsorbate is much more pronounced. The present estimation in the case of an isolated Pd atom correlates fairly well with that by Matveev *et al.*[22] In the case of an extended deposit, the increase of electronic population of the Pd atom directly at the vacancy is accompanied by a decrease at the neighboring Pd. Although the horizontal range of vacancy-induced modifications clearly excedes the (2×2) cell, its vertical modifications are principally limited to the interface layer, the second Pd layer being only slightly modified.

Although the precise electronic occupations are probably not entirely meaningful, the present results show clearly that oxygen vacancies are at the origin of an enhanced electron transfer from the substrate towards the deposit. The electrons transferred remain well localized on the atom at the vacancy site, which receives additional electrons from its metal neighbors of the interfacial layer. Taking this into account, we expect that the modification of the reactivity suggested

already for the catalysis for the isolated adatoms[23] may in fact concern only extremely flat clusters or edges and corners of three-dimensional clusters. In the direction perpendicular to the interface, the modification of the electronic occupations remains fairly localized to the interface region and it is likely that the effect of the vacancy site will be completely screened for the case of a three-dimensional deposit. This observation seems to be in agreement with the results of Sanchez *et al.*,[20] where, although the oxidation process takes place on a three-dimensional cluster, the key vacancy-induced modification of the dissociation barrier happens at the edge atom adsorbed directly at the vacancy.

V. CONCLUSIONS

We have used the DFT-based, periodic *ab initio* electronic band-structure method to study the influence of surface oxygen vacancies on the characteristics of palladium deposition on the MgO (100) surface.

For the isolated Pd adatoms, we find a strong increase of adsorption energy and an important electron transfer from the substrate to the adsorbate. The perfect agreement of the present findings with the existing cluster results shows the full equivalence of the two approaches for the description of the surface processes.

For more extended deposits, the stabilizing effect of vacancies attenuates quite rapidly. Its strong dependence on the coordination of the deposited metal atoms suggests that vacancies will preferably occupy regions at the cluster's edges and corners. With regard to the electron redistribution at the interface, we find that the strong electron transfer from the substrate to the deposit remains also for more extended deposits. In all cases, however, the transferred electrons remain very well localized on the Pd atom at the vacancy. One can thus expect that the major vacancy-induced modification of the reactivity would be limited to those metal atoms at the cluster edges that adsorb directly at the vacancies. Either direct or indirect effects on the other atoms of a three-dimensional particle should be relatively small.

ACKNOWLEDGMENTS

We thank C. Henry and G. Tréglia for their interest and for helpful discussions during the course of this work. The most time consuming calculations were performed on the NEC-SX5 computer at IDRIS, under Project No. 960732. We are grateful for a generous allocation of time on the machine. The work of L.G. and G.P. has been supported by the Italian INFM through the PRA-ISADORA project. The CRMC^2 is also associated with the Universities of Aix-Marseille II and III.

[1] V. E. Henrich and P. A. Cox, *The Surface Science of Metal Oxides* (Cambridge University Press, Cambridge, 1994).
[2] C. Noguera, *Physics and Chemistry at Oxide Surfaces* (Cambridge University Press, Cambridge, 1995).
[3] G. Bordierc and C. Noguera, Phys. Rev. B **44**, 6361 (1991).
[4] F. Didier and J. Jupille, Surf. Sci. **314**, 378 (1994).
[5] M.W. Finnis, J. Phys.: Condens. Matter **8**, 5811 (1996).
[6] C.R. Henry, Surf. Sci. Rep. **31**, 231 (1998).
[7] G. Renaud, Surf. Sci. Rep. **32**, 1 (1998).
[8] H.J. Freund, Faraday Discuss. **114**, 1 (1999).
[9] H.J. Freund, H. Kuhlenbeck, and V. Staemmler, Rep. Prog. Phys. **59**, 283 (1996).
[10] C. Duriez, C. Chapon, C.R. Henry, and J.M. Rickard, Surf. Sci. **230**, 123 (1990).
[11] V. Musolino, A. Selloni, and R. Car, J. Chem. Phys. **108**, 5044 (1998).
[12] I.V. Yudanov, G. Pacchioni, K.M. Neyman, and N. Rösch, J. Phys. Chem. B **101**, 2786 (1997).
[13] N. Lopez and F. Illas, J. Phys. Chem. **102**, 1430 (1998).
[14] N. Lopez, F. Illas, N. Rösch, and G. Pacchioni, J. Phys. Chem. **110**, 4873 (1999).
[15] A. Bogicevic and D.R. Jennison, Surf. Sci. **437**, L741 (1999).
[16] D. Fuks, S. Dorfman, E.A. Kotomin, Y.F. Zhukovskii, and A.M. Stoneham, Phys. Rev. Lett. **85**, 4333 (2000).
[17] *Chemisorption and Reactivity on Supported Clusters and Thin Films*, edited R.M. Lambert and G. Pacchioni (Kluwer Academic Publishers, Dordrecht, 1997).
[18] G. Pacchioni, Surf. Rev. Lett. **7**, 277 (2000).
[19] G. Haas, A. Menck, H. Brune, J.V. Barth, J.A. Venables, and K. Kern, Phys. Rev. B **61**, 11 105 (2000).
[20] A. Sanchez, S. Abbet, U. Heiz, W.-D. Schneider, H. Häkkinen, R.N. Barnett, and U. Landmann, J. Phys. Chem. A **103**, 9573 (1999).
[21] A.M. Ferrari and G. Pacchioni, J. Phys. Chem. **100**, 9032 (1996).
[22] A.V. Matveev, K.M. Neyman, I.V. Yudanov, and N. Rösch, Surf. Sci. **426**, 123 (1999).
[23] S. Abbet, A. Sanchez, U. Heiz, W.-D. Schneider, A.M. Ferrari, G. Pacchioni, and N. Rösch, J. Am. Chem. Soc. **122**, 3453 (2000).
[24] Yu F. Zhukovskii, E.A. Kotomin, P.W.M. Jacobs, A.M. Stoneham, and J.H. Harding, J. Phys.: Condens. Matter **12**, 55 (2000).
[25] P. Blaha , K. Schwarz , and J. Luitz , WIEN97, Vienna University of Technology, 1997 [improved and updated Unix version of the original copyrighted WIEN code, which was published by P. Blaha, K. Schwarz, P. Sorantin, and S. B. Trickey, Comput. Phys. Commun **59**, 399 (1990)] .
[26] C. Li, R-q. Wu, A.J. Freeman, and C.L. Fu, Phys. Rev. B **48**, 8317 (1993).
[27] R-q. Wu and A.J. Freeman, Phys. Rev. B **51**, 5408 (1995).
[28] K. Carling, G. Wahnstrom, T.R. Mattsson, A.E. Mattsson, N. Sandberg, and G. Grimvall, Phys. Rev. Lett. **85**, 3862 (2000).
[29] D.R. Jennison and A. Bogicevic, Surf. Sci. **464**, 108 (2000).
[30] J. Goniakowski, Phys. Rev. B **58**, 1189 (1998).
[31] J.P. Perdew, K. Burke, and Y. Wang, Phys. Rev. B **54**, 16 533 (1996).
[32] J. Goniakowski and C. Noguera, Phys. Rev. B **60**, 16 120 (1999).
[33] F. Finocchi, J. Goniakowski, and C. Noguera, Phys. Rev. B **59**, 5178 (1999).
[34] L.N. Kantorovich, J.M. Holender, and M.J. Gillan, Surf. Sci. **343**, 221 (1995).
[35] G. Pacchioni and P. Pescarmona, Surf. Sci. **412/413**, 657 (1998).

[36] E. Scorza, U. Birkenheuer, and C. Pisani, J. Phys. Chem. **107**, 9645 (1997).
[37] P.V. Sushko, A.L. Shluger, and C.R.A. Catlow, Surf. Sci. **450**, 153 (2000).
[38] I.V. Yudanov, S. Vent, K.M. Neyman, G. Pacchioni, and N. Rösch, Chem. Phys. Lett. **275**, 245 (1997).
[39] J. Goniakowski, Phys. Rev. B **57**, 1935 (1998).
[40] O. Robach, G. Renaud, and A. Barbier, Phys. Rev. B **60**, 5858 (1999).
[41] A.M. Flank, R. Delaunay, P. Lagarde, M. Pompa, and J. Jupille, Phys. Rev. B **53**, R1737 (1996).
[42] L. Giordano, J. Goniakowski, and G. Pacchioni (unpublished).
[43] H. Graoui, S. Giorgio, and C.R. Henry (unpublished).
[44] J. Goniakowski, Phys. Rev. B **59**, 11 047 (1999).
[45] R.F.W. Bader, Chem. Rev. **91**, 983 (1991).